

# Conformation and Aggregation Behavior of Poly(ethylene glycol)-*b*-Poly(lactic acid) Amphiphilic Copolymer Chains in Dilute/Semidilute THF Solutions

Bingjian Yao,<sup>1</sup> Qingzeng Zhu,<sup>1</sup> Hui Liu,<sup>1</sup> Liang Qiao,<sup>1</sup> Jingcheng Hao,<sup>1,2</sup> Feng Qi<sup>3</sup>

<sup>1</sup>Key Laboratory of Special Functional Aggregated Materials, Ministry of Education, School of Chemistry and Chemical Engineering, Shandong University, Jinan 250100, China

<sup>2</sup>Key Laboratory for Colloid and Interface Chemistry, Ministry of Education, School of Chemistry and Chemical Engineering, Shandong University, Jinan 250100, China

<sup>3</sup>Qilu Hospital of Shandong University, Jinan 250100, China

Received 24 August 2011; accepted 30 November 2011

DOI 10.1002/app.36613

Published online in Wiley Online Library (wileyonlinelibrary.com).

**ABSTRACT:** The behavior of amphiphilic copolymer chains in a solvent is not the same as that of homopolymers. As an important synthetic biomaterial, poly(ethylene glycol)-*b*-poly(lactic acid) copolymers are often dissolved in tetrahydrofuran (THF) for study. Few studies have focused on the potential aggregation behavior and compact conformation of the amphiphilic macromolecules in a THF solution. In this study, a series of poly(ethylene glycol)-*b*-poly(lactic acid) diblock copolymers were synthesized and characterized using fourier-transform infrared spectroscopy, nuclear magnetic resonance, thermogravimetric analysis, and gel permeation chromatography methods. The aggregation behavior of amphiphilic molecular chains in a THF solution was studied using dynamic light scattering

and transmission electron microscopy. The results showed that the aggregation size in solutions at a concentration of 2.0 mg/mL is within the range of 50–250 nm. It was further demonstrated that molecular chains exhibit a compact conformation in a dilute THF solution, which leads to a comparatively larger deviation in the characterization of molecular weights using GPC method. Here, a model is proposed to elucidate the dynamic evolution between compact amphiphilic single chains and aggregates. © 2012 Wiley Periodicals, Inc. *J Appl Polym Sci* 000: 000–000, 2012

**Key words:** biomaterials; diblock copolymer; transmission electron microscopy; dynamic light scattering; gel permeation chromatography

## INTRODUCTION

Amphiphilic copolymers are built by joining two or more parts that have different solubility and chemical properties. The behavior of amphiphilic copolymer molecular chains in a solution is not the same as that of homopolymers. The specific state mainly depends on their chemical structure and solvent quality. Amphiphilic copolymers are known to self-

assemble into large variety of aggregate morphologies in selective media.<sup>1–22</sup> In aqueous solutions, for example, the association of the hydrophobic segments results in a certain degree of aggregation, whereas the water-soluble chains extend into the bulk aqueous phase.<sup>23,24</sup> Amphiphilic diblock copolymers have been experimentally observed to assemble into vesicles and rod- or sphere-like micelles in water depending on manipulation procedures.<sup>25,26</sup> Poly(ethylene oxide)-*b*-poly(propylene oxide),<sup>27,28</sup> poly(ethylene oxide)-*b*-poly(butadiene),<sup>29,30</sup> poly(ethylene oxide)-*b*-polytetrahydrofuran,<sup>31</sup> poly(ethylene oxide)-*b*-poly(*N*-isopropylacrylamide), and poly(ethylene oxide)-*b*-poly(vinyl alcohol)<sup>32–34</sup> exhibit self-assembling behavior in aqueous solution. Recently, research has focused on a type of biodegradable and biocompatible amphiphilic copolymer that includes poly(ethylene oxide)-*b*-poly(caprolactone) and poly(ethylene oxide)-*b*-poly(lactic acid).<sup>35–37</sup> These polymers come into use as sutures, staples, and scaffolds in tissue engineering and for the controlled release of drugs because of the amphiphilic properties and the advantages of these homopolymers.<sup>38–42</sup> Research on morphogenesis of poly(ethylene oxide)-*b*-poly(caprolactone) in aqueous media has been performed.<sup>43–45</sup> Li studied the behavior of poly(ethylene oxide)-*b*-

Correspondence to: Q. Zhu (qzzhu@sdu.edu.cn).

Contract grant sponsor: Natural Science Foundation of China; contract grant number: 20404006.

Contract grant sponsor: Shandong Province Natural Science Foundation; contract grant number: ZR2009BM038.

Contract grant sponsor: China Postdoctoral Science Foundation; contract grant number: 20090461212.

Contract grant sponsor: Science and Technology Development Planning of Shandong province; contract grant number: 2009GG20003016.

Contract grant sponsor: Independent Innovation Foundation of Shandong University IIFSDU; contract grant number: 2011JC012.

Contract grant sponsor: National Basic Research Program of China; contract grant number: 2009CB930103.

*Journal of Applied Polymer Science*, Vol. 000, 000–000 (2012)  
© 2012 Wiley Periodicals, Inc.

polylactide block copolymers in aqueous solutions.<sup>46</sup> The block copolymers are susceptible to form micelles because of their hydrophobic polylactide segments.

When block copolymers are dissolved in nonselective solvents (solvents appropriate for all blocks), the copolymers are generally considered to exist as single chains. Because of the unfavorable thermodynamic interactions between different blocks, the aggregated conformation of single polymer chains was observed in some investigated systems, such as poly(ethylene oxide)-*b*-poly(*N,N*-dimethylacrylamide) copolymers in water and tetrahydrofuran (THF),<sup>47</sup> poly(ethylene oxide)-*b*-poly(methyl methacrylate) in THF, acetone, chloroform and 2,2,2-trifluoroethanol,<sup>48</sup> polystyrene-*b*-polyisoprene copolymers in bis(2-ethylhexyl) phthalate solution,<sup>49,50</sup> polystyrene-*b*-poly(*N*-vinylpyrrolidone) copolymers in methanol solution,<sup>51</sup> and block copolymers of polystyrene and quaternized poly(*N,N*-diethylamino)isoprene in *N,N*-dimethylformamide, dioxane, and THF solutions.<sup>52</sup>

It is difficult to find a solvent with the same solubility for each segment of an amphiphilic copolymer, even if the solvent can dissolve both segments. A good solvent condition for one segment may not be appropriate for the other segments. In other words, the solvent toward one segment may encourage copolymer chains to form association states.<sup>53,54</sup> THF is often used as a solvent for poly(ethylene oxide)-*b*-poly(lactic acid) copolymers (PEG-PLA).<sup>55–57</sup> However, few studies have focused on the potential aggregation behavior and compact conformation of PEG-PLA amphiphilic copolymer chains in THF solutions. In this study, a series of PEG-PLA copolymers with fixed PEG segments of  $2.0 \times 10^3$  g/mol were synthesized and characterized. The conformation and aggregation behavior of amphiphilic PEG-PLA copolymer chains in dilute and semidilute THF solutions were studied.

## EXPERIMENTAL

### Materials

D,L-Lactide was purchased from Chengdu Organic Chemicals. Monomethoxy poly(ethylene glycol) (PEG) was obtained from Sigma-Aldrich ( $M_n = 2.0 \times 10^3$  g/mol). Stannous octoate was supplied by Sinopharm Chemical Reagent Company. Methanol, dichloromethane and diethyl ether from Tianjin Guangcheng Chemical Reagent Company, were analytical grade. THF was HPLC grade.

### Measurements

Fourier-transform infrared spectroscopy (FTIR) was performed on a Bruker TENSOR27 spectrometer in the range of 4000 to 400  $\text{cm}^{-1}$  to identify the struc-

ture of synthesized copolymers. Each sample was prepared for an FTIR analysis by casting a 2.0 wt %  $\text{CH}_2\text{Cl}_2$  solution onto KBr windows. The sample was then placed in an oven at 50°C for 48.0 h under vacuum to completely remove solvent.  $^1\text{H}$  nuclear magnetic resonance ( $^1\text{H-NMR}$ ) spectra were recorded on a 400 MHz UltraShield<sup>TM</sup> magnet (Bruker) spectrometer using  $\text{CDCl}_3$  as a solvent. Chemical shifts ( $\delta$ ) are given in ppm using tetramethylsilane as an internal reference. Thermogravimetric analysis (TGA) was performed using a Mettler TGA/ADTA851<sup>e</sup> thermal analyzer. The samples (6.0–10.0 mg) were heated from ambient temperature to 600°C at a heating rate 10°C/min under an inert atmosphere of nitrogen. Gel permeation chromatography (GPC) equipped with a Waters 515 system, a 2410 refractive index detector and two Styragel gel columns was calibrated with narrow-molecular-weight polystyrene (PS) standards and was used to characterize the molecular weight of the synthesized copolymers. THF was used as a mobile phase at a flow rate of 1.0 mL/min. The concentrations of samples were in the range of 2.0–3.0 mg/mL and the injection volume was 100  $\mu\text{L}$  for each analysis. The columns and detector were maintained at 35°C.

Dynamic light scattering (DLS) experiments were performed to measure the hydrodynamic radius ( $R_h$ ) of particles on a Brookhaven BI-200SM instrument using a solid-state laser (200 mW,  $\lambda = 632$  nm). The temperature was controlled at 25°C. The scattered light was collected on a Brookhaven BI-9000 AT correlator. Intensity time correlation functions  $g^{(2)}(\tau)$  were recorded in the angular range from 20° to 95°, and the evaluation of the hydrodynamic radius was obtained using the Laplace inversion program CONTIN. The THF solution of PEG-PLA was first filtered through 0.22  $\mu\text{m}$  Millipore filter to remove dust particles. Transmission electron microscopy (TEM) was performed on a JEM-1400 electron microscope (JEOL) operated at an accelerating voltage of 120 kV. Specimens were prepared by dipping a copper grid into THF solutions of copolymers. The grid was then left to stand on a piece of filter paper and air dried before measurement.

### Preparation of PEG-PLA copolymers

PEG-PLA copolymers with fixed PEG segments were synthesized by ring-opening polymerization of D,L-lactide in the presence of PEG ( $2.0 \times 10^3$  g/mol). In brief, appropriate amounts of D,L-lactide and PEG were mixed in a 100 mL three-necked round-bottom flask. The flask was evacuated under vacuum for 2.0 h to remove trace water. Subsequently, 0.5 wt % stannous octoate was added. Polymerization was performed at 140–145°C for 12.0 h under nitrogen atmosphere. For purification, the resulting

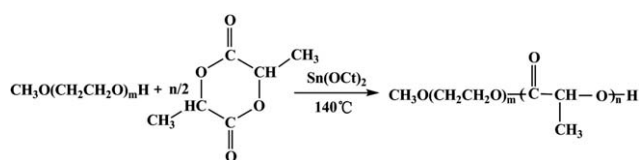


Figure 1 Synthetic route of PEG-PLA copolymers.

copolymer was dissolved in  $\text{CH}_2\text{Cl}_2$  and then precipitated in excess cold methanol or diethyl ether. The PEG-PLA copolymers were filtered and dried at room temperature under vacuum.

## RESULTS AND DISCUSSION

### Characterization of PEG-PLA copolymers

The synthetic route of the PEG-PLA copolymers, which is a ring-opening polymerization reaction, is shown in Figure 1. Table I presents the PEG-PLA copolymers synthesized with different feeding ratios of D,L-lactide to PEG. The theoretic molecular weights are in the range of  $7.0 \times 10^3$  to  $7.2 \times 10^4$  g/mol. The copolymers synthesized were confirmed using FTIR. The absorption bands at 2990, 2876, and  $1380 \text{ cm}^{-1}$  are attributed to the methyl groups. The peaks at 2930 and  $1460 \text{ cm}^{-1}$  are due to methylene groups and are clearly observable. The characteristic peaks at 1750 and  $1187 \text{ cm}^{-1}$  indicate the existence of ester groups, and the strong absorption peak at  $1091 \text{ cm}^{-1}$  is assigned to the ether (C—O—C) group.

$^1\text{H-NMR}$  measurements were used to determine the chemical structure of PEG-PLA. Figure 2 shows the  $^1\text{H-NMR}$  spectrum of specimen 3. Peaks at 5.200 and 1.566 ppm are attributed to the  $^1\text{H}$  of tertiary carbon and methyl groups, respectively, in the PLA block. The peak at 3.645 ppm is characteristic of methylene groups in PEG segments. The peaks at

TABLE I  
Comparison of Molecular Weights of PEG-PLA Copolymers Obtained by Different Methods

PEG-PLA	$M_n^{\text{a}}$	NMR		GPC	
		$M_n^{\text{b}}$	$M_n$	$M_w$	PD <sup>c</sup>
1	7001	6477	4500	6200	1.37
2	12,007	11,847	4800	7400	1.52
3	22,012	22,265	5300	9000	1.69
4	31,999	37,245	5400	8700	1.56
5	51,985	55,613	5800	8600	1.48
6	72,029	72,963	11,800	24,800	2.09

<sup>a</sup>  $M_n^{\text{a}}$ : theoretic molecular weight of PEG-PLA copolymers calculated according to feeding ratios of D,L-lactide to PEG.

<sup>b</sup>  $M_n^{\text{b}}$ : molecular weight of PEG-PLA obtained by examining the ratio of integrals of  $^1\text{H}$  resonances of CH group in PLA ( $\delta = 5.200 \text{ ppm}$ ) to that of  $\text{CH}_2\text{CH}_2\text{O}$  group in PEG segments ( $\delta = 3.645 \text{ ppm}$ ) according to eq. (1).

<sup>c</sup> PD: polydispersity of PEG-PLA copolymers determined by GPC.

3.42 and 4.37 ppm are attributed to terminal methoxy hydrogen protons and methylene protons connected to ester structural units, respectively.

### Molecular-weight characterizations

The integrations of the  $^1\text{H-NMR}$  peaks at 3.645 and 5.200 ppm, which belong to the PEG and PLA segments, respectively, can be used to calculate the number-average molecular weight ( $M_n$ ) of PEG-PLA copolymers. The molecular weight of the PEG segment is known to be  $2.0 \times 10^3$  g/mol, which can be used as an internal standard in the determination of the average molecular weight of PEG-PLA diblock copolymers. The molecular weights of the PLA segments were determined by an examination of the ratio of methine protons (CH) in the PLA segment to

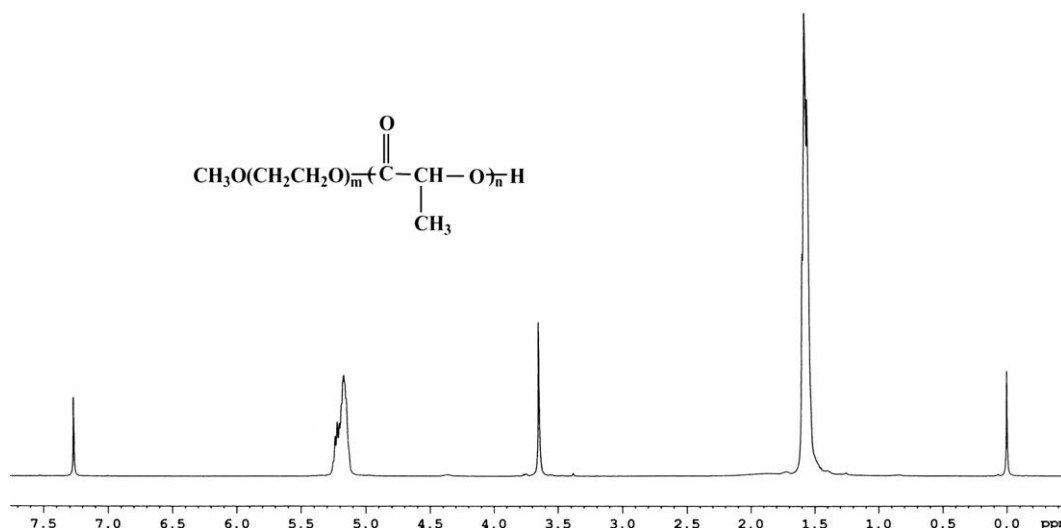


Figure 2  $^1\text{H-NMR}$  spectrum of PEG-PLA copolymer (specimen 3).

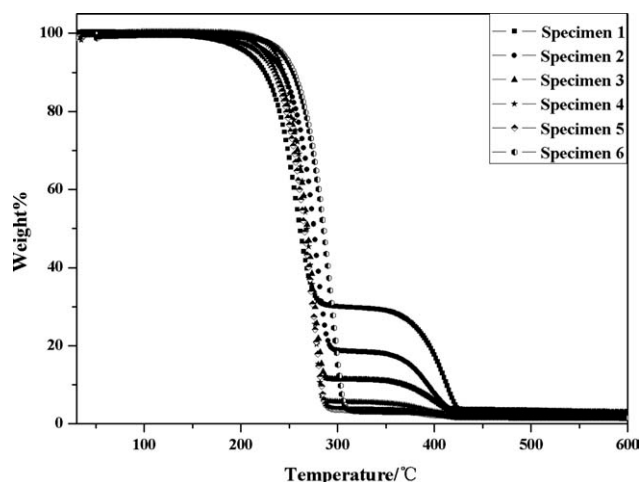


Figure 3 TGA curves of PEG-PLA copolymers.

methylene (CH<sub>2</sub>) protons in the PEG segment. The  $M_n$  of the PEG-PLA copolymers summarized in Table I was obtained according to eq. (1). The table shows that the  $M_n$  determined using <sup>1</sup>H-NMR is in good agreement with the theoretic molecular weight ( $M_n^0$ ) calculated from the D,L-lactide/PEG feeding ratios.

$$M_n = \overline{DP}_{mPEG} \times 4 \times \frac{\text{Integration (CH)}}{\text{Integration (CH}_2\text{)}} \times 72 + \overline{DP}_{mPEG} \times 44 \quad (1)$$

Here, Integration (CH) and Integration (CH<sub>2</sub>) represent the integrals of <sup>1</sup>H resonances of CH group in PLA and CH<sub>2</sub>CH<sub>2</sub>O group in PEG segments, respectively.

Moreover, the average molecular weights and molecular-weight distribution of polymers can be obtained using the GPC method, and their values are considered to be relative to the narrow-dispersed-polymer standards used for calibration of the system. Table I presents a survey of the molecular-weight data of PEG-PLA copolymers based on the GPC analysis. The resulting molecular weights are much smaller than those obtained by the <sup>1</sup>H-NMR method. However, the GPC analysis shows positive relationship with the D,L-lactide/PEG feed ratios.

TABLE II  
TGA Data of PEG-PLA Copolymers

PEG-PLA	$M_n^0$	Theoretical weight loss (%)		Experimental weight loss (%)	
		Step1	Step 2	Step 1	Step 2
1	7001	71.43	28.57	70.64	28.72
2	12,007	83.33	16.67	82.31	14.91
3	22,012	90.91	9.09	89.68	8.08
4	31,999	93.75	6.25	93.49	4.45
5	51,985	96.15	3.85	95.92	2.23
6	72,029	97.22	2.78	96.19	2.65

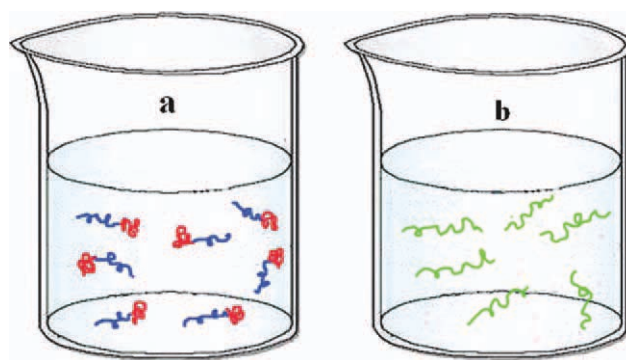


Figure 4 Schematic illustration of chain conformation in a dilute THF solution: (a) PEG-PLA; (b) polystyrene, (Blue line represents PEG segment; red line represents PLA segment; green line represents polystyrene chains). [Color figure can be viewed in the online issue, which is available at [wileyonlinelibrary.com](http://wileyonlinelibrary.com).]

In this work, TGA was performed to estimate molecular segments of the PEG-PLA diblock copolymers. For block copolymers, TGA curves can show different breakdown stages because of the dissimilar thermal stability of each segment. Consequently, the quantitative analysis of block copolymer compositions can be performed using this method. PEG-PLA copolymers contain polyester and polyether segments, and the PLA segment is bound through an ester linkage to the PEG segment. In the TGA curves of PEG-PLA copolymers, two thermal degradation stages were observed (Fig. 3). Because the ether bond is more stable than the ester group, PEG segments break down at high temperature. The thermal analysis data are summarized in Table II. The PEG and PLA segment weights in the PEG-PLA specimens calculated according to the TGA curves are in reasonable agreement with those obtained using the <sup>1</sup>H-NMR method. For example, in the TGA curve,

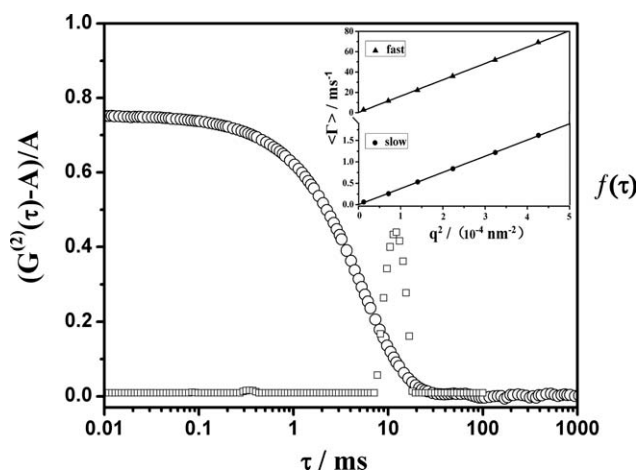
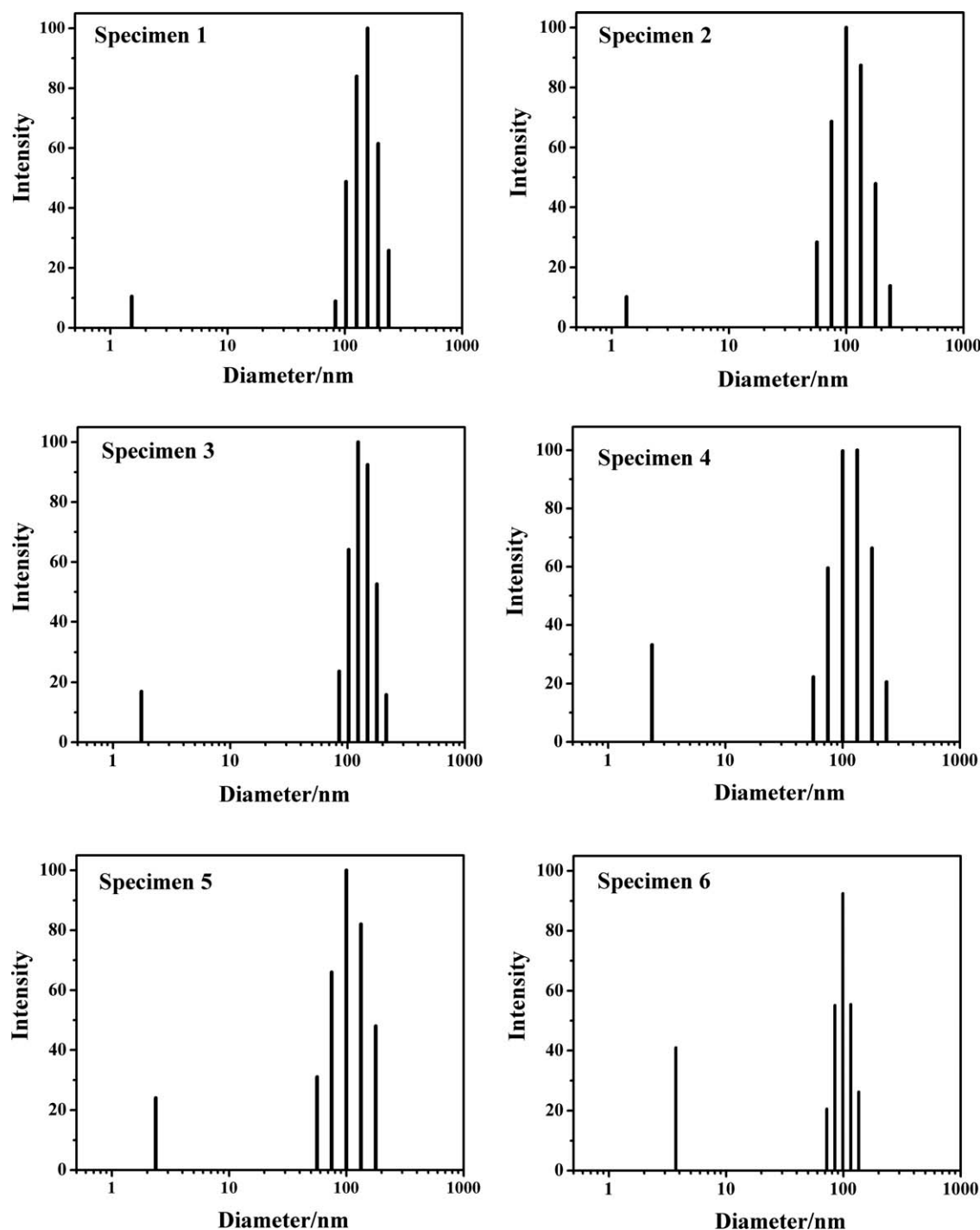


Figure 5 Selected correlation function  $g^{(2)}(\tau)$  and corresponding relaxation time distributions of specimen 3 at 20°. Inset is dependence of relaxation rates on the square of the scattering vector ( $q^2$ )



**Figure 6** Hydrodynamic radius ( $R_h$ ) distributions of PEG-PLAs in THF solutions obtained using dynamic light scattering.

the two step weight losses of specimen 3 are 89.68 and 8.08%, respectively. The theoretic PLA and PEG contents of specimen 3 are 90.91 and 9.09%.

#### Compact chain conformation

GPC primarily uses conventional liquid-chromatographic equipment. A polymer solution flows through a column or series of columns that contain

a special gel with pores comparable in size to the molecular coils in the solution. As the polymer molecules elute from the columns, they are separated by the scale of their hydrodynamic radius and then detected using a suitable concentration detector to produce an elution volume curve (concentration vs. time). A distribution can be produced because the instrument has been calibrated using narrow-dispersed polymer standards. By suitable data

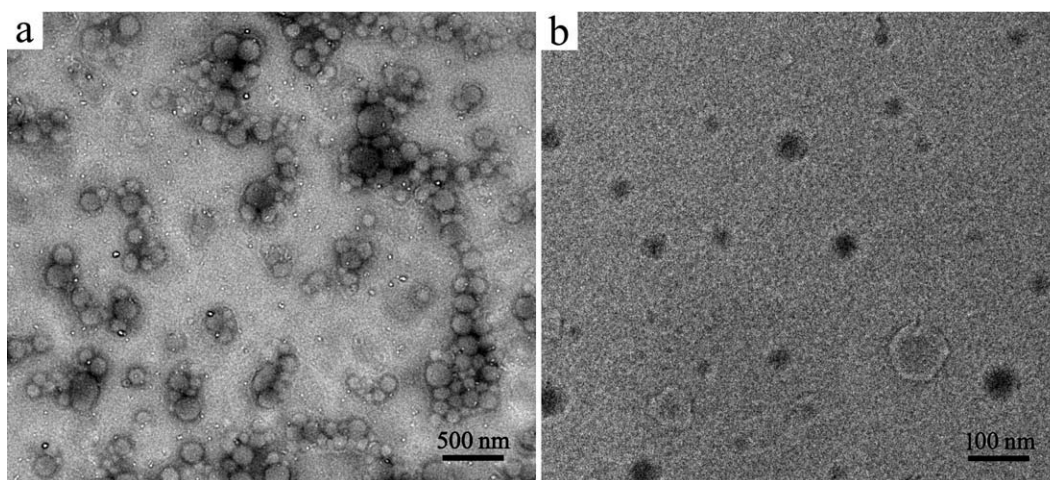


**Figure 7** Representative TEM images of specimen 3 in a semidilute THF solution. (a) in the solution kept a static state for 48.0 h; (b) in the fresh prepared THF solution.

manipulation, average molecular weights can be calculated. The mechanism of the GPC instrument is based on size-exclusion theory. Clearly, the molecular weights determined using GPC are closely related to the chain conformation of samples in dilute solution and the narrow standards.

The solubility parameters ( $\zeta$ ) of THF, PLA, PEG, and PS are  $18.6 \text{ MPa}^{1/2}$ ,  $21.3 \text{ MPa}^{1/2}$ ,  $19.9 \text{ MPa}^{1/2}$ , and  $18.6 \text{ MPa}^{1/2}$ , respectively.<sup>58</sup> PS shows the same  $\zeta$  as THF and has uniformity and consistency within the entire chain. Accordingly, PS has a good degree of stretch and a high excluded volume in a THF solution. PEG has a  $\zeta$  similar to that of THF. The large  $\Delta\zeta$  (solubility parameter gap) between PLA and THF indicates that PLA has a comparatively poor solubility in THF. Therefore, in a dilute THF solution, the PLA segments tend to curl, which results in a compact PEG-PLA chain conformation and the decline of apparent excluded volume (see Fig. 4). When compared with PS chains, PEG-PLA chains will exhibit a crimp conformation and smaller coils in a dilute THF solution, which causes deviation of PEG-PLA molecular weights determined by GPC using narrow-dispersed PS standards. These results may explain why the molecular weights of PEG-PLA determined using GPC are significantly lower than the theoretic values.

### Aggregation

To gain insight into the behavior of PEG-PLA molecular chains in a semidilute solution, DLS experiments were performed. PEG-PLA copolymers were dissolved in THF at a concentration of  $2.0 \text{ mg/mL}$ , which was the same as the initial sample concentration used for GPC measurements. The sample solutions were kept a static state for 48.0 h prior to measurement. Intensity time correlation functions  $g^{(2)}(\tau)$

were recorded in the angular range from  $20^\circ$  to  $95^\circ$ . Figure 5 shows a typical experimental intensity correlation function  $g^{(2)}(\tau)$  for specimen 3 measured at  $20^\circ$ , together with the corresponding relaxation time distributions. The relaxation time distribution is found to be bimodal with a fast and slow mode relaxation peaks. Both relaxation rates are linearly dependent on the square of the scattering vector ( $q$ ) and pass through the origin, showing that both modes are diffusive. The fast diffusive mode is attributed to the unimers and the the slow mode is attributed to the aggregates formed by PEG-PLA in THF solution. The apparent hydrodynamic radius  $R_h$  of the majority particles computed according to the CONTIN method was in the range of 50–250 nm (Fig. 6). These particles are in an aggregation state formed by the association of several PEG-PLA chains. A small quantity of particles with hydrodynamic radii of several nanometers was also found in the solutions. This size represents a typical diameter of a single chain. As reported in the literature, the  $R_h$  of single poly ( $\alpha$ -methylstyrene) chains with  $M_w$  of  $1.3 \times 10^4$  and  $2.48 \times 10^4 \text{ g/mol}$  in a good solvent are 2.66 and 3.66 nm, respectively.<sup>59</sup> From the results of DLS, the aggregates and single molecular chains clearly coexist in the THF solution, and the aggregates of multichains are the primary structure form.

**TABLE III**  
Dynamic Light Scattering Results of PEG-PLA Copolymers in Fresh Prepared THF Disperse Systems

Concentration (mg/mL)	$R_h$ (nm)	
	Specimen 3	Specimen 6
2.5	29.9	44.1
2.0	27.7	42.2
1.5	28.3	45.6
0.5	28.7	44.0

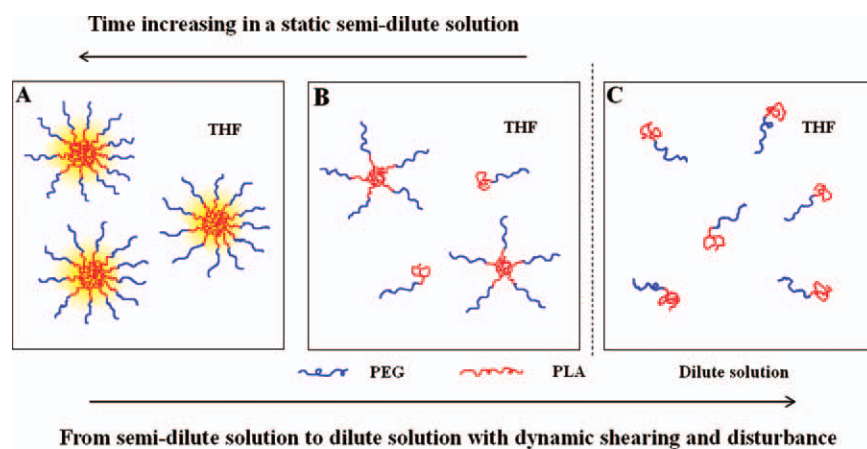


**Figure 8** A schematic model of PEG-PLA chains behavior in a semidilute THF solution and a dilute THF solution. [Color figure can be viewed in the online issue, which is available at [wileyonlinelibrary.com](http://wileyonlinelibrary.com).]

To provide direct evidence for the aggregation behavior of PEG-PLA in THF solution predicted by DLS measurements, TEM measurements were performed to observe possible aggregation morphology. Figure 7 shows a typical TEM image of specimen 3 in a semidilute solution. The spherical aggregates, which exhibit diameters in the range of 50–250 nm, are visualized clearly [Fig. 7(a)]. These results are in good agreement with those determined using DLS.

In the fresh prepared THF solutions, the  $R_h$ s of specimen 3 and specimen 6 with different concentrations were measured using DLS (Table III). The average values of the  $R_h$ s were 28.6 and 44.0 nm, respectively. These values are smaller than the  $R_h$ s detected in solutions equilibrated for 48.0 h. Furthermore, at the experimental concentrations, the scale of the aggregates showed little change when concentrations were increased from 0.5 to 2.5 mg/mL. This phenomenon can be explained as follows: in a fresh THF solution, initial aggregates assisted by hydrophobic interaction of PLA blocks are formed. This process is a spontaneous. In this stage, the scale of the aggregates does not depend on the concentration. With time, other PEG-PLA chains will enter into the aggregates and the aggregates will grow larger. Furthermore, some copolymer chains and solvent molecules are embedded in the inner core of the micelle-like structures. Consequently, the  $R_h$  detected will result in larger values and present some degree of dispersion. Because of the longer hydrophobic PLA segments, the  $R_h$  of specimen 6 is larger than that of specimen 3 in the freshly disperse system. Figure 7(b) shows the morphology obtained from a fresh solutions of specimen 3.

In summary, in a semidilute THF solution, the association of hydrophobic PLA segments results in a certain degree of aggregation of PEG-PLA molecular chains. PLA segments form a core, with the PEG segments stretched out and forming a “brush” at the

periphery of the core. State “A” in Figure 8 illustrates the aggregation behavior of PEG-PLA chains in a static semidilute THF solution. When the system is disturbed, such as by flowing through the GPC system, where the porous particles wall dynamically shear the chains and the chains are diluted by the mobile phase, the structure of multichains will dis-aggregate. After the solution elutes from the GPC columns, the PEG-PLA chains will be compact single chains dispersed in THF and described as state “C”. State “B” is an intermediate state between “A” and “C”. A compact single coil of PEG-PLA in a dilute THF solution will give a small molecular weight characterized using GPC.

## CONCLUSIONS

THF is often used as a solvent for PEG-PLA amphiphilic copolymers. The solution of PEG-PLA in THF is commonly dealt with as a homogenous solution. The potential behavior of aggregated conformation is ignored. This study demonstrates that multichain aggregates and single chains of PEG-PLA coexist in a semidilute THF solution. Multichain aggregates can be disaggregated by dilution effect together with the interaction of dynamic shear and disturbanc. The PEG-PLA chains present a compact conformation in a dilute THF solution, which leads to a comparatively larger deviation in the characterization of molecular weights using the GPC method. These results on PEG-PLA amphiphilic copolymers in THF solutions can be used for reference to consider other amphiphilic copolymers solutions in so-called good solvents.

## References

1. Astafieva, I.; Zhong, X. F.; Eisenberg, A. *Macromolecules* 1993, 26, 7339.

2. Liu, T.; Liu, L. Z.; Chu, B. In *Amphiphilic Block Copolymers: Self-Assembly and Applications*; Alexandridis, P., Lindman, B.; Eds.; Elsevier: Amsterdam, 2000.
3. Bronich, T. K.; Vinogradov, S. V. *Nano Lett* 2001, 1, 535.
4. Kukula, H.; Schlaad, H.; Antonietti, M.; Forster, S. *J Am Chem Soc* 2002, 124, 1658.
5. Schuch, H.; Klingler, J.; Rossmann, P.; Frechen, T.; Gerst, M.; Feldthusen, J.; Müller, A. H. E. *Macromolecules* 2000, 33, 1734.
6. Ding, J. F.; Liu, G. J.; Yang, M. L. *Polymer* 1997, 38, 5497.
7. Blanz, A.; Madsen, J.; Battaglia, G.; Ryan, A. J.; Armes, S. P. *J Am Chem Soc* 2011, 133, 16581.
8. Riess, G. *Prog Polym Sci* 2003, 28, 1107.
9. Xu, R. L.; Winnik, M. A.; Hallett, F. R.; Riess, G.; Croucher, M. D. *Macromolecules* 1991, 24, 87.
10. Won, Y. Y.; Ted Davis, H.; Bates, F. S. *Science* 1999, 283, 960.
11. Li, Z. B.; Kesselman, E.; Talmon, Y.; Hillmyer, M. A.; Lodge, T. P. *Science* 2004, 306, 98.
12. Cui, H. G.; Chen, Z. Y.; Zhong, S.; Wooley, K. L.; Pochan, D. J. *Science* 2007, 317, 647.
13. Wang, X. S.; Guerin, G.; Wang, H.; Wang, Y. S.; Manners, I.; Winnik, M. A. *Science* 2007, 317, 644.
14. Christian, D. A.; Tian, A. W.; Ellenbroek, W. G.; Levental, I.; Raiagopal, K.; Janmey, P. A.; Liu, A. J.; Baumgart, T.; Discher, D. E. *Nat Mater* 2009, 8, 843.
15. Jiang, Y.; Zhu, J. T.; Jiang, W.; Liang, H. J. *J Phys Chem B* 2005, 109, 21549.
16. Tang, X. Z.; Hu, Y. C.; Pan, C. J. *Polymer* 2007, 48, 6354.
17. Zhang, W. Q.; Shi, L. Q.; An, Y. L.; Gao, L. C.; Wu, K.; Ma, R. *J Macromolecules* 2004, 37, 2551.
18. Ræz, J.; Manners, I.; Winnik, M. A. *J Am Chem Soc* 2002, 124, 10381.
19. Nuopponen, M.; Ojala, J.; Tenhu, H. *Polymer* 2004, 45, 3643.
20. Yang, H.; Jia, L.; Zhu, C. H.; Di-Cicco, A.; Levy, D.; Albouy, P. A.; Li, M. H.; Keller, P. *Macromolecules* 2010, 43, 10442.
21. Yao, J.; Ravi, P.; Tam, K. C.; Gan, L. H. *Langmuir* 2004, 20, 2157.
22. Giacomelli, G.; Schmidt, V.; Aissou, K.; Borsali, R. *Langmuir* 2010, 26, 15734.
23. Gohy, J. F. *Adv Polym Sci* 2005, 190, 65.
24. Liu, Y.; Xu, Q.; Liu, P.; El Ghzaoui, A.; Li, S. M. *Int J Pharmaceut* 2010, 394, 43.
25. Zhang, L.; Eisenberg, A. *Science* 1995, 268, 1728.
26. Luo, L.; Eisenberg, A. *Langmuir* 2001, 17, 6804.
27. Almgren, M.; Brown, W.; Hvidt, S. *Colloid Polym Sci* 1995, 273, 2.
28. Chu, B.; Zhou, Z. *Surfact Sci Ser* 1996, 60, 67.
29. Won, Y. Y.; Brannan, A. K.; Ted Davis, H.; Bates, F. S. *J Phys Chem B* 2002, 106, 3354.
30. Jain, S.; Bates, F. S. *Science* 2003, 300, 460.
31. Yang, Y. W.; Deng, N. J.; Yu, G. E.; Zhou, Z. K.; Attwood, D.; Booth C. *Langmuir* 1995, 11, 4703.
32. Motokawa, R.; Morishita, K.; Koizumi, S.; Nakahira, T.; Annaka, M. *Macromolecules* 2005, 38, 5748.
33. Yan, J. J.; Ji, W. X.; Chen, E. Q.; Li, Z. C.; Liang, D. H. *Macromolecules* 2008, 41, 4908.
34. Zhou, J. H.; Ke, F. Y.; Tong, Y. Y.; Li, Z. C.; Liang, D. H. *Soft Matter* 2011, 7, 9956.
35. Clapper, J. D.; Skeie, J. M.; Mullins, R. F.; Guymon, C. A. *Polymer* 2007, 48, 6554.
36. Siao, W. Y.; Lin, L. H.; Chen, W. W.; Huang, M. H.; Chong, P. *J Appl Polym Sci* 2009, 114, 509.
37. Yu, L.; Zhang, Z.; Zhang, H.; Ding, J. *Biomacromolecules* 2009, 10, 1547.
38. Li, S.; Vert, M. *Macromolecules* 2003, 36, 8008.
39. Govender, T.; Riley, T.; Ehtezazi, T.; Garnett, M. C.; Stolnik, S.; Illum, L.; Davis, S. S. *Int J Pharmaceut* 2000, 199, 95.
40. Molina, I.; Li, S. M.; Martinez, M. B.; Vert, M. *Biomaterials* 2001, 22, 363.
41. Liggins, R. T.; Burt, H. M. *Adv Drug Deliver Rev* 2002, 54, 191.
42. Ruana, G.; Feng, S. S. *Biomaterials* 2003, 24, 5037.
43. Yan, G.; Discher, D. E. *Polymer* 2006, 47, 2519.
44. Du, Z. X.; Xu, J. T.; Fan, Z. Q. *Macromolecules* 2007, 40, 7633.
45. Zupancich, J. A.; Bates, F. S.; Hillmyer, M. A. *Macromolecules* 2006, 39, 4286.
46. Liu, Y.; Zhao, Z.; Wei, J.; Ghzaoui, A. E.; Li, S. *J Colloid Interface Sci* 2007, 314, 470.
47. Ke, F.; Mo, X.; Yang, R.; Wang, Y.; Liang, D. *Macromolecules* 2009, 42, 5339.
48. Edelmann, K.; Janich, M.; Hoinkis, E.; Pyckhout-Hintzen, W.; Horing, S. *Macromol Chem Phys* 2001, 202, 1638.
49. Hanley, K. J.; Lodge, T. P.; Huang, C. I. *Macromolecules* 2000, 33, 5918.
50. Hanley, K. J.; Lodge, T. P. *J Polym Sci Part B: Polym Phys* 1998, 36, 3101.
51. Hussain, H.; Tan, B. H.; Gudipati, C. S.; He, C. B.; Liu, Y.; Davis, T. P. *Langmuir* 2009, 25, 5557.
52. Riegel, I. C.; Samios, D.; Adi Eisenberg, C. L. *Polymer* 2003, 44, 2117.
53. Schmidt, R.; Pamies, R.; Kjøniksen, A. L.; Zhu, K.; Hernández Cifre, J. G.; Nyström, B.; García de la, T. *J Phys Chem B* 2010, 114, 8887.
54. Xie, D. H.; Xu, K.; Bai, R. K.; Zhang, G. Z. *J Phys Chem B* 2007, 111, 778.
55. Ding, H. Y.; Sumer, B. D.; Kessinger, C. W.; Dong, Y.; Huang, G.; Boothman, D. A.; Gao, J. M. *J Controlled Release* 2011, 151, 271.
56. Xiong, J.; Meng, F. H.; Wang, C.; Cheng, R.; Liu, Z.; Zhong, Z. Y. *J Mater Chem* 2011, 21, 5786.
57. Wei, Q.; Li, T.; Wang, G. L.; Li, H.; Qian, Z. Y.; Yang, M. H. *Biomaterials* 2010, 31, 7332.
58. Pu, Z. C.; Lu, L. C.; Mikos, A. G. In *Polymer Data Handbook*; Mark, J. E., Ed.; Oxford University Press: New York, 1999; p 542.
59. Tominaga, Y.; Suda, I.; Osa, M.; Yoshizaki, T.; Yamakawa, H. *Macromolecules* 2002, 35, 1381.